Meteorol Atmos Phys
DOI 10.1007/s00703-014-0324-6

ORIGINAL PAPER

Contributions of solar and greenhouse gases forcing during the present warm period

Hyung-Gyu Lim · Sang-Wook Yeh · Ji-Won Kim · Rokjin Park · Chang-Keun Song

Received: 14 November 2013 / Accepted: 31 March 2014

Abstract Due to the dramatic increase in the global mean surface temperature (GMST) during the twentieth century, the climate science community has endeavored to determine which mechanisms are responsible for global warming. By analyzing a millennium simulation (the period of 1000–1990 AD) of a global climate model and global climate proxy network dataset, we estimate the contribution of solar and greenhouse gas forcings on the increase in GMST during the present warm period (1891–1990 AD). Linear regression analysis reveals that both solar and greenhouse gas forcing considerably explain the increase in global mean temperature during the present warm period, respectively, in the global climate model. Using the global climate proxy network dataset, on the other hand, statistical approach suggests that the contribution of greenhouse gas forcing is slightly larger than that of solar forcing to the increase in global mean temperature during the present warm period. Overall, our result indicates that the solar forcing as well as the anthropogenic greenhouse gas forcing plays an important role to increase the global mean temperature during the present warm period.

Responsible editor: S. Hong.

H.-G. Lim
School of Environmental Science and Engineering, POSTECH, Pohang, Korea

S.-W. Yeh (✉)
Department of Marine Sciences and Convergent Technology, Hanyang University, ERICA, Seoul, Korea
e-mail: swyeh@hanyang.ac.kr

J.-W. Kim
Department of Atmospheric Sciences, Yonsei University, Seoul, Korea

R. Park
School of Earth and Environmental Sciences, Seoul National University, Seoul, Korea

C.-K. Song
Department of Climate and Air Quality, National Institute of Environmental Research, Seoul, Korea

1 Introduction

The global mean surface temperature (GMST) gradually increased during the twentieth century. According to the Intergovernmental Panel on Climate Change (IPCC) Fourth Assessment Report (Trenberth et al. 2007), the GMST increased by approximately 0.74 ± 0.18 °C between the years 1906 and 2005. Based on observations and model simulations, furthermore, many previous studies argue that global warming has been continuous (Tett et al. 1999; Meehl et al. 2005).

The effects of natural and greenhouse gas (GHG) forcings on such the global increase in temperature have been estimated in many studies (Beer et al. 2000; Meehl et al. 2003; Scafetta and West 2006; Lean and Rind 2008; Schwartz et al. 2010). There is no doubt that the climate science community is endeavoring to address which mechanism is primarily responsible for global warming. Specifically, investigations are focusing on how much natural external forcing or GHG forcing explains recent and ongoing increases in the GMST. It is believed that the increased concentration of GHG plays a key role to increase GMST since the industrial period. Carbon dioxide (CO_2) and methane (CH_4) are the primary GHG species except water vapor that directly influences the GMST, specifically by increasing the longwave radiative flux from

Published online: 12 June 2014

the atmosphere to the surface of Earth (Trenberth et al. 2007). In addition to the GHG forcings, however, radiative forcings due to such as external solar forcing and internal volcanic forcing may be responsible for the variations of GMST (Lean et al. 1995; Crowley and Kim 1996; Free and Robock 1999; Tett et al. 1999; Bertrand et al. 2002; Bauer et al. 2003; Cho et al. 2012). This perspective is mostly based on the facts that the actual contribution of GHG forcings to changes the radiative budget is unclear and natural external forcings other than GHG forcings may be useful in explaining some of the variability in GMST on decadal-to-centennial timescales.

Among them, it has been suggested that solar forcing, which increases over the twentieth century, may be an alternative explanation for the GMST variations (Lean et al. 1995; Rind et al. 2004; Song et al. 2010). High correlations between solar forcing and climate variability have been shown to exist on time scales ranging from the 11-year solar cycle to many millennia, and it has been suggested that solar forcing could be an important driver of GMST (Mann et al. 1998; Beer et al. 2000; Crowley 2000; Douglass and Clader 2002; Scafetta and West 2006). Interestingly, recent studies have shown that even the relatively short-term 11-year solar cycle forcing can amplify the climate system (Reid 1997; Meehl et al. 2009; Misios and Schmidt 2012) and also ultraviolet irradiance variations to speculate that a solar cycle could have influence on regional winter temperatures using a model study since 2003 (Ineson et al. 2011).

Although the aforementioned studies provide useful individual insights about the global climate, the relative contributions of natural, in particular, solar forcing, and GHG forcings to changes in the GMST are still unclear. The climate science community attempts to overcome this deficiency by using climate model simulations and/or paleo-climate proxy data. To estimate the relative contribution of natural and GHG forcings during the present warm period, we analyze ECHO-G coupled general circulation model (CGCM) which is forced by both natural and GHG forcings covering 1000–1990 AD called ERIK simulation (Gonzalez-Rouco et al. 2003; Zorita et al. 2003, 2005; von Storch et al. 2004; Min et al. 2005a, b; Liu et al. 2009; Xueyuan et al. 2011). Furthermore, we also use a global climate proxy network dataset provided by Mann et al. (2008) to compare with the results obtained by the ERIK simulation. Details of the ERIK simulation and global climate proxy network dataset are discussed in Sect. 2.

It is known that anomalous warm climate occurred around AD 950–1250, which is called medieval warm period, although the concentration of greenhouse gases is low and almost fixed during those periods in comparison with the present warm period (Hughes and Diaz 1994; Crowley and Lowery 2000; Mann 2002; Mann et al. 2009). That is, the medieval warm period is similar to the present warm period except but the concentration of GHG. In the ERIK simulation, specifically, we compare the two different warm periods, i.e., the medieval warm period and the present warm period. While the natural forcing maybe responsible for the variations of GMST during the medieval warm period, both the natural and GHG forcing may be responsible for the warming of GMST during the present warm period. By calculating the relationship between the GMST and solar forcing during the both periods, we estimate how much natural forcing and GHG forcing explains the variations of GMST during the present warm period. Furthermore, we also use a statistical approach, i.e., Monte Carlo methodology, to estimate the contribution of solar forcing and GHG forcing using the global climate proxy network dataset and then we compare the former with the latter.

2 Data and ERIK simulation validation

The coupled model used in this study is the ECHO-G model, which consists of the spectral atmospheric model ECHAM4 coupled with the global ocean circulation model HOPE-G using the OASIS coupler. Both models were developed and implemented at the Max-Planck Institute for Meteorology in Hamburg (Legutke and Voss 1999). The configuration used for this simulation has 39 vertical levels, including 19 in the atmosphere and 20 in the ocean, and horizontal resolutions of 3.75° (atmosphere) and 2.8° (ocean) in both latitude and longitude. The millennial integration for the period 1000–1990 AD includes a forced run (called ERIK simulation) (Zorita et al. 2005), which was forced by three natural external forcing factors: solar variability, greenhouse gases concentrations in the atmosphere including CO_2 and CH_4, and an estimated radiative effect of stratospheric volcanic aerosols. In the ERIK simulation, the radiative flux at the top of the atmosphere is calculated to include the effects of sunspots and cosmic ray isotopes (Crowley 2000; von Storch et al. 2004). Also included, the effect of volcanic ash on radiation forcing is first estimated based on the concentration of sulfides in the Greenland ice core and then calculated by the atmospheric model (Robock and Free 1996; Crowley 2000). On the other hand, a global climate proxy network dataset (hereafter, we will refer to as climate proxy data) comprises more than a thousand tree-ring, ice core, coral, sediment, and other assorted proxy records spanning the ocean and land regions of both hemispheres over the past 1,500 years. The surface temperature field is reconstructed by calibrating the proxy network against the spatial information contained within

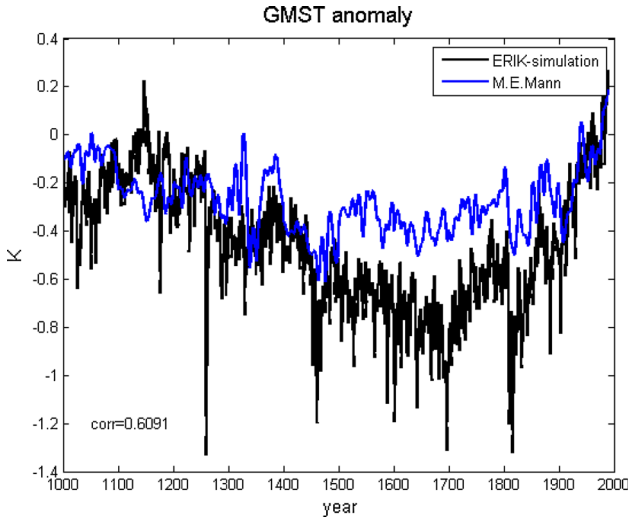

Fig. 1 Time series of the global mean surface temperature anomaly obtained by the ERIK simulation (*black line*) and the global climate proxy network dataset from Mann et al. (2009) (*blue line*) for the period of 1000–1990 AD. Anomalies are defined relative to the 1961–1990 reference period mean

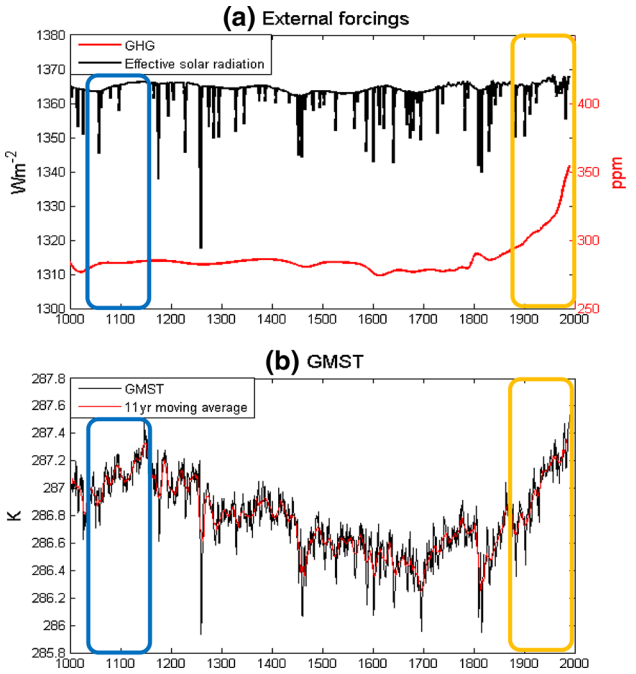

Fig. 2 **a** The time series of effective solar radiation (*black*) and the concentration of greenhouse gases used in the ERIK simulation. Note that the *y*-axis for the greenhouse gases is indicated on the *right side*. **b** The time series of the global mean surface temperature anomaly simulated in the ERIK model (*black*) and its 11-year running mean (*red*). The *yellow* and *blue boxes* in (**a**) and (**b**) highlight the medieval warm period (1051–1150) and the present warm period (1891–1990)

the instrumental annual mean surface temperature field (Brohan et al. 2006)over a modern period of overlap between proxy and instrumental data (1850–1995) using the RegEM CFR procedure (Mann et al. 2007)with additional minor modifications. Details of this dataset are described by Mann et al. (2008, 2009).

To validate the model performance, we compare the time series of GMST anomalies simulated in the ERIK simulation with that derived from a global climate proxy network dataset (Fig. 1). The GMST time series generated from the ERIK simulation is correlated with that obtained from the climate proxy data. A simultaneous correlation coefficient between the two time series is 0.60 for the period of 1000–1990 AD, which is statistically significant at the 95 % confidence level. However, for the little ice age period of 1400–1700 AD, the ERIK simulation shows much colder GMSTs than those derived from the climate proxy data. In contrast, the ERK simulation shows warmer GMST than the climate proxy data for the medieval warm period. According to previous study, on the other hand, the ERIK simulation reasonably captures the last 1,000 years of surface air temperature variation over China as deduced from the proxy data according to previous study (Liu et al. 2009). Thus, although certain discrepancies exist between the GMST simulated by the ERIK simulation and those derived from the climate proxy data, the ERIK simulation is useful to examine the contribution of natural and GHG forcing to changes in the GMST between the medieval warm period and the present warm period.

3 Contribution of solar and GHG forcing during the present warm period

The time sequences of two main forcings in the ERIK simulation, i.e., the effective radiative forcings which consider the total solar irradiance with stratospheric volcanic aerosols effects (Crowley 2000), and the GHG concentration for the period of 1000–1990 AD, are displayed in Fig. 2a. In this context, the effective radiative effects are used to represent the sum of the solar constant and the volcanic forcing. That is, the volcanic forcing is parameterized as a simple reduction of the annual-mean solar constant, starting in the year with a volcanic eruption and its effect usually lasts a couple of years according to the reconstructions of volcanic aerosol forcing (Crowley 2000). Figure 2b shows the time series of the average GMST from the ERIK simulation (black line) along with an 11-year running mean time series of GMST (red line). The GHG concentration is a relatively constant 270–280 ppm until the nineteenth century, after which it dramatically increases, especially after the mid-nineteenth century, to 350 ppm at the end of the twentieth century. The GMST most significantly and consistently increases during the period of 1891–1990, i.e., the present warm

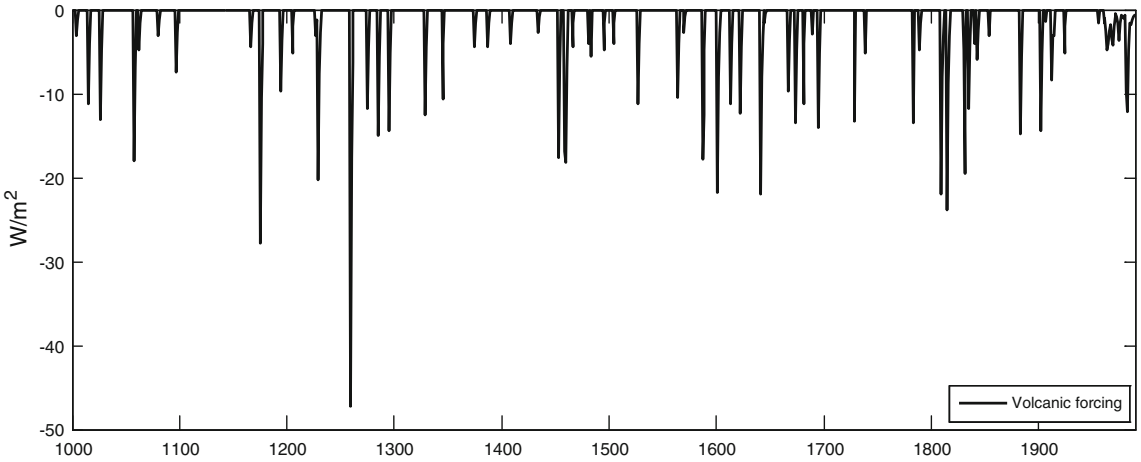

Fig. 3 The time series of volcanic forcing in ERIK simulation

period (orange box in Fig. 2b). However, the GMST also rapidly increases during the period of 1051–1150, i.e., the medieval warm period (blue box in Fig. 2b). That is, two epochs of significant increases in GMST exist during the last 1,000 years.

The most striking difference between the two epochs of increasing GMST is that the concentration of GHG is much lower during the medieval warm period than during the present warm period, as simulated by the ERIK model. The mean GHG concentration during the medieval warm period is 282.5 ppm, which is lower than the 325.1 ppm concentration during the present warm period. In addition, the GHG concentration changes very little during the medieval warm period, but it constantly and significantly increases throughout the present warm period (Fig. 2a). The zero-order hypothesis is that the physical mechanism responsible for the GMST increase differs between the two epochs. In other words, the GMST change during the medieval warm period may originate from natural forcings, rather than forced climate change from GHG emission, as suggested by a previous study (Crowley and Lowery 2000). In contrast, the increase in GMST during the present warm period might be due to both an increase in GHG concentration and natural forcing.

In order to estimate how much of the change in GMST is explained by the solar and GHG forcing, respectively, we first examine the relationship between GMST variation and solar forcing in each of the two epochs. It should be noted that we exclude years with volcanic forcing. The years with volcanic forcing are defined when the volcanic forcing is above 0 W/m^2 (Fig. 3). In the ERIK simulation, the volcanic forcing is the maximum when the volcanic eruption occurs and then it approaches 0 W/m^2 2 or 3 years later from the volcanic eruption year. Figure 4a plots GMST against solar forcing during the medieval warm period, and GMST changes linearly with solar forcing. During the medieval warm period, GMST ranges 286.7–287.5 K and solar forcing ranges 1,363–1,366 W/m^2. A linear regression analysis confirms that GMST increases with solar forcing at a rate of 0.086 K/(W/m^2), which is statistically significant at the 95 % confidence band. We also plot solar forcing against the GHG concentration during the medieval warm period in Fig. 4b, which shows that the GHG concentration remains nearly constant around 283 ppm in spite of considerable variations in solar forcing as shown in Fig. 4a. Combined, these results indicate that the change in the solar forcing is mainly associated with the GMST variations during the medieval warm period. Moreover, because there is little change in the greenhouse gas concentration during the medieval warm period, we can consider the rate of GMST change due to solar forcing to be 0.086 K/(W/m^2) in the ERIK simulation.

Figure 4c, d is the same as Fig. 4a, b but for the present warm period. Similar to that during the medieval warm period, the GMST during the present warm period changes linearly with changes in solar forcing (Fig. 4c). However, in contrast to the relationship seen during the medieval warm period, changes in the concentration of GHG are also linearly related to the variation in solar forcing (Fig. 4d) during the present warm period. This indicates that increases in the GMST during the present warm period are related both to changes in solar forcing and in the GHG concentration. The GMST during the present warm period varies in the range of 286.8–287.3 K, which is comparable to the range of GMST change during the medieval warm period. The range of solar forcing during the present warm period, namely 1,365–1,368 W/m^2, is also similar to that during the medieval warm period. However, a liner regression coefficient to explain the relationship between solar forcing and GMST change during the present warm period becomes larger (i.e., 0.156 K/(W/m^2)) than that during the medieval warm period. We argue that the rate of

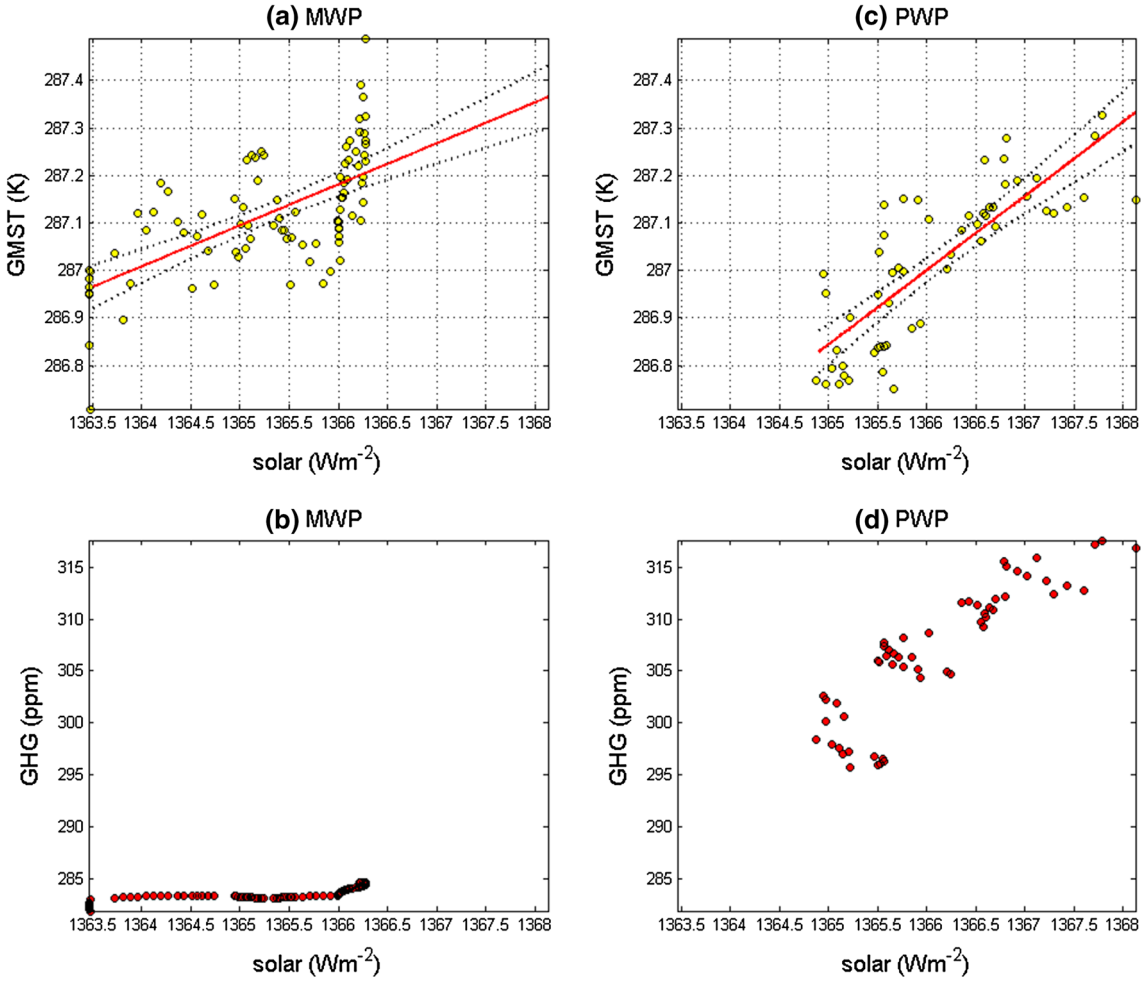

Fig. 4 **a** Scatter plot of solar forcing versus GMST variation in the medieval warm period. The *red line* indicates the regression coefficient and the *black dashed line* indicates the 95 % confidence band. **b** is the same as (**a**) but for greenhouse gases instead of solar forcing. **c** and **d** are the same as (**a**) and (**b**) but for the present warm period

0.156 K/(W/m^2) during the present warm period is not due to the solar forcing only. That is, the increase in GHG concentration is also responsible for the increase in GMST during the present warm period. Note that the concentration of GHG increases significantly from 295–316 ppm during the present warm period. Therefore, it is needed to isolate the GHG forcing in the rate of 0.156 K/(W/m^2) during the present warm period. To isolate the GHG forcing from the increase in GMST during the present warm period, we use the sensitivity due to solar forcing during the medieval warm period [i.e., 0.086 K/(W/m^2)], which may represent the contribution of solar forcing absent any significant change in GHG concentration. By subtracting the sensitivity coefficient from both periods, we can estimate the contribution of GHG forcing during the present warm period. The result shows that the sensitivity of GMST to GHG forcing during the present warm period is 0.070 K/(W/m^2), which indicates that solar forcing and GHG forcing may explain 56 and 44 % of the increase in GMST during the present warm period, respectively.

In addition, we remove GHG forcing from GMST using the linear relationship of solar forcing and GHG and it is found that the contribution of solar forcing on GMST variations is 0.079 K/(W/m^2) during the medieval warm period. The result indicates that solar forcing and GHG forcing may explain 51 and 49 % of the increase in GMST during the present warm period, respectively.

From now on, we analyze the climate proxy data to examine the contribution of natural and GHG forcing based on a statistical methodology. The purpose of this analysis is to examine a range of the contribution of natural and GHG forcing during the present warm period. We analyze different periods in the ERIK simulation and climate proxy dataset to examine the uncertainty of solar forcing contribution on the GMST variations during the present warm period. Note that the ERIK simulation is forced by three

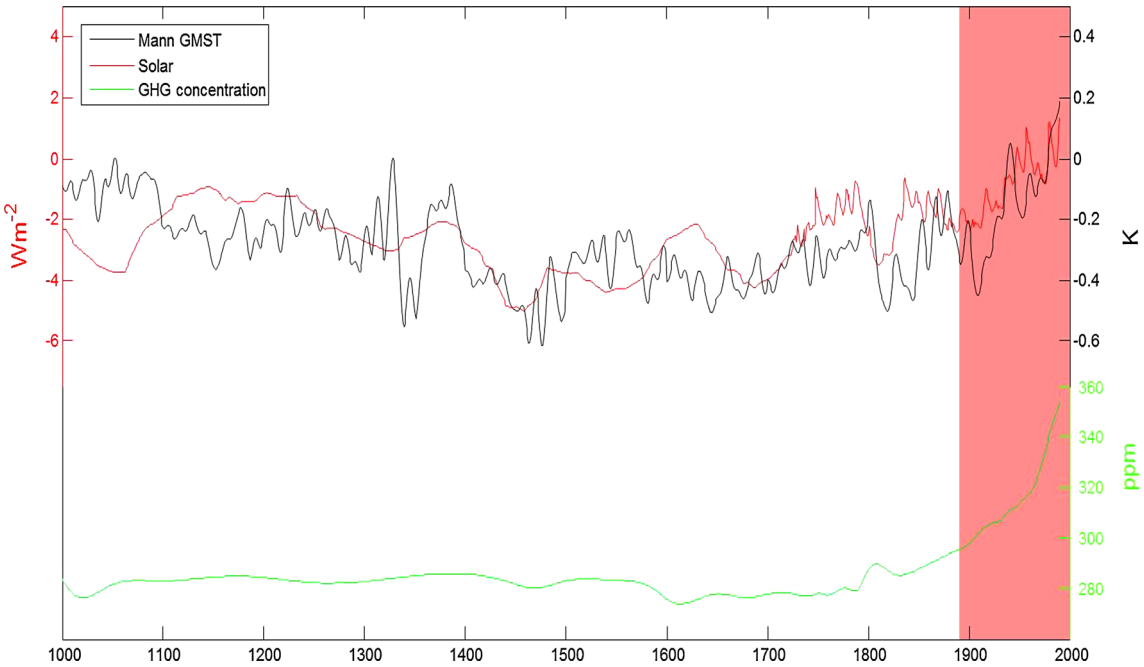

Fig. 5 Time series of anomalous global mean surface temperature in the global climate proxy network dataset (*black line*) from Mann et al. (2009), total solar irradiance (*red line*) from Crowley (2000) and GHG concentration (*green line*) in the period of 1000–1990, respectively. *Red box* indicates the present warming period (i.e., 1891–1990).Anomalies for the global mean surface temperature and total solar irradiance are defined relative to the 1961–1990 reference period mean. Note that the *y*-axis for the anomalous global mean surface temperature and the GHG concentration is indicated on the right side

natural external forcings, which might be different from the observations, i.e., the climate proxy data. In addition, the climate proxy data are not available in the polar region which is contrast to the ERIK simulation. These may lead a different rate of GMST change due to solar forcing between the climate proxy data and the ERIK simulation .

Figure 5 displays the variations of GMST in the period of 1000–1900 (black line in Fig. 5) obtained by the climate proxy data along with the variations of solar forcing obtained from Crowley (2000) (red line in Fig. 5). Using these two time series, we also estimate the relative contribution of solar forcing and the GHG forcing using Monte Carlo methodology. That is, we randomly select a sample of 100 year in the period of 1000–1800 when the concentration of GHG is nearly constant (green line in Fig. 5). Note that the variations of solar forcing and the concentration of GHG are obtained from the ERIK simulation. From a randomly selected 100-year sample out of 801 year (1000–1800), we calculate the relationship between the increase in GMST and that in solar forcing based on a linear regression analysis as conducted in the ERIK simulation. Note that we again exclude the years when solar forcing is influenced by volcanic events in the entire period. And then we repeat this process as many as 10,000 times by allowing the randomly selected years to obtain the probability density function of the linear regression coefficients as shown in Fig. 6.

It is found that the mean rate of GMST change due to solar forcing is about 0.04 K/(W/m^2) $\pm$ 0.01 in the period of 1000–1800 in the climate proxy data. To obtain the probability density function on the mean rate of GMST due to solar forcing during the present warm period (Fig. 6b), we apply the same regression analysis as in Fig. 6a. In other words, we randomly select a sample of 100 years in the present warm period (i.e., 1891–1990) and then we calculate the linear regression coefficients between the increase in GMST and that in solar forcing. The rate of GMST change due to solar forcing is 0.1 K/(W/m^2) $\pm$ 0.01 in the period of 1891–1990, which is larger than that during the pre-industrial period. Note that the rate of 0.1 K/(W/m^2) $\pm$ 0.01 is slightly low with 0.156 K/(W/m^2) in ERIK simulation because the climate proxy data are not available in the polar region. In addition, the ERIK simulation is forced by three natural external forcings such as solar forcing, greenhouse gas forcing, and the estimated radiative forcing due to stratospheric volcanic aerosols, which might be different from the observations, i.e., the climate proxy data. Similar to the ERIK simulation, we argue that the rate of 0.1 K/(W/m^2) during the present warm period is not due to the solar forcing only; thus, the increases in the GMST during the present warm period might be due to both the changes in solar forcing and in the GHG concentration. Comparing with the two values of rates (i.e., 0.04 K/(W/m^2) $\pm$ 0.01 versus 0.1 K/(W/m^2)), we are able to estimate the contribution of solar

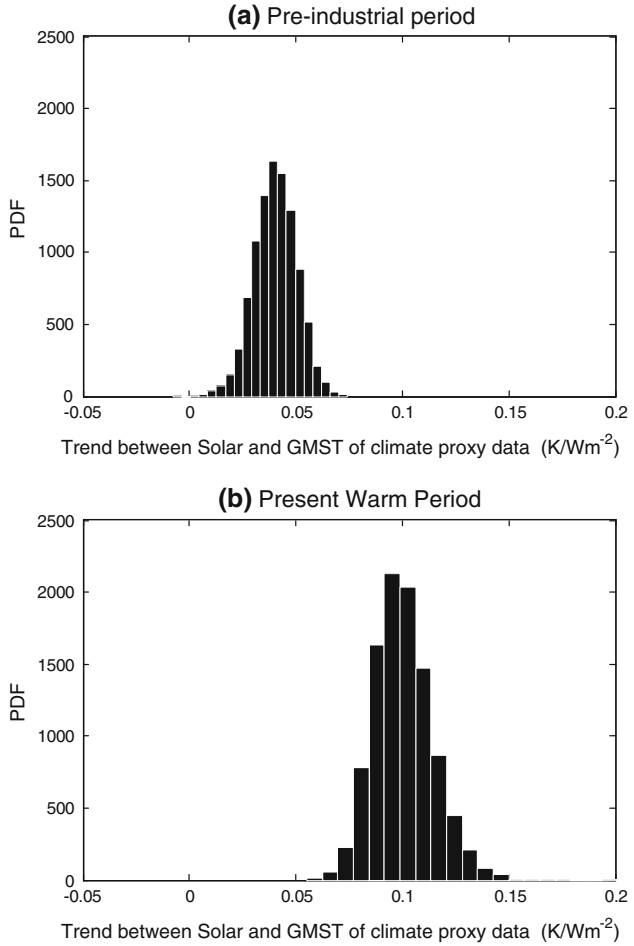

Fig. 6 Probability density function of linear regression coefficients of solar forcing versus GMST of (**a**) pre-industrial period (1000–1800) and (**b**) Present warm period (1891–1990) in the global climate proxy network dataset using Monte Carlo approach. See the text for the details of methodology

forcing and GHG forcing to the changes in GMST during the present warm period is around 30 $\sim$ 50 % and 50 $\sim$ 70 %, respectively, in the climate proxy data. In comparison with the ERIK simulation, it turns out that the GHG forcing contributes more to the variations of GMST during the present warm period in the climate proxy data.

4 Summary

The response of the climate system to natural and GHG forcing depends on complex feedback mechanisms associated with clouds, water vapor, ice cover, and land characteristics (Beer et al. 2000). Therefore, it is difficult to isolate the contribution of natural and GHG forcing on GMST variability. By analyzing a millennium simulation (the period of 1000–1990 AD) in a global climate model forced by both natural forcing and GHG forcing (i.e., ERIK simulation) and the climate proxy data, we estimated the contribution of solar forcing and GHG forcing to the increase in GMST during the present warm period.

In particular, we compared between the changes of GMST during two different periods (i.e., the medieval warm period (1051–1150) and present warm period (1891–1990)) which have similar warm trends in spite of a large difference of the GHG concentration in the two periods of the ERIK simulation. It is found that GMST increases with solar forcing at a rate of 0.086 K/(W/m^2) during the medieval warm period. Because the GHG concentration is relatively constant during the medieval warm period, we can consider 0.086 K/(W/m^2) to be the sensitivity of the increase in GMST to solar forcing in the ERIK simulation. Based on these results, we concluded that the solar and greenhouse gases forcings explain 56–60 % and 40–44 % of the increase in GMST during the present warm period, respectively. That is, both solar and greenhouse gas forcing explain the increase in global mean temperature during the present warm period, respectively, in the global climate model.

Using the climate proxy data, on the other hand, we suggested that solar forcing explains 30 $\sim$ 50 % and GHG forcings explain 50 $\sim$ 70 % of the increase in GMST during the present warm period, respectively. Interestingly, the contribution of solar forcing during the present warm period is similar to previous studies using the climate proxy data. For example, Scafetta and West (2006) argued that the sun contributed as much as 45 $\sim$ 50 % of the 1900–2000 global warming and Beer et al. (2000) also argued that solar forcing is responsible for about 40 % of the increase in GMST during the past 140 years. However, it should be noted that solar irradiance data are highly uncertain for the preindustrial period, which may affect the estimate of solar forcing contribution presented in this study. For example, Lean and Rind (2008) argued that solar forcing contributed 10 % of the warming in the past 100 years and also mentioned the uncertainty of solar forcing. Therefore, this might explain partly the reason why the results in the present study is different from major conclusion of the recent IPCC AR5 (Stocker et al. 2013) showing that the solar forcing is negligible in the total radiative forcing to induce the global warming compared to greenhouse forcings and short-lived climate pollutant forcings. The contribution of solar forcing during the present warm period is high in the ERIK simulation, which might be associated with the fact that the ERIK simulation is only forced by solar, volcanic and the two GHG forcings. Overall, these results serve to highlight the important contribution of solar forcing as well as the GHG forcing to the increase in GMST during the present warm period.

Acknowledgments We acknowledge Dr. S.-Y. Yim at IPRC for providing the ERIK simulation data sets. This work is supported by

Korea Ministry of Environment as "Climate Change Correspondence Program" and S.-W. Yeh is also supported from the Brain Korea 21 Plus Project in Department of Marine Sciences and Convergent Technology of Hanyang University.

References

Bauer E, Claussen M, Brovkin V, Huenerbein A (2003) Assessing climate forcings of the Earth system for the past millennium. Geophys Res Lett 30(6):1276. doi:10.1029/2002GL016639

Beer J, Mende W, Stellmacher R (2000) The role of the sun in climate forcing. Quat Sci Rev 19:403–415

Bertrand C, Loutre MF, Crucifix M, Berger A (2002) Climate of the last millennium : a sensitivity study. Tellus 54A:221–224

Brohan P, Kennedy JJ, Harris I, Tett SFB, Jones PD (2006) Uncertainty estimates in regional and global observed temperature changes: a new dataset from 1850. J Geophys ResAtmos 111:D12106. doi:10.1029/2005JD006548

Cho IH, Kwak YS, Chang HY, Cho KS, Kim YH, Park YD (2012) The global temperature anomaly and solar North-South asymmetry. Asia-Pacific J Atmos Sci 48(3):253–257

Crowley TJ (2000) Causes of climate change over the past 1000 years. Science 289:270–277. doi:10.1126/science.289.5477.270

Crowley TJ, Kim KY (1996) Comparison of proxy records of climate change and solar forcing. Geophys Res Lett 23:359–362

Crowley TJ, Lowery TS (2000) How warm was the medieval warm period? A comment on 'man-made versus natural climate change'. AMBIO 29(1):51–54. doi:10.1579/0044-7447-29.1.51

Douglass DH, Clader BD (2002) Climate sensitivity of the earth to solar irradiance. Geophys Res Lett 29NO 16. 10.1029/2002GL015345

Free M, Robock A (1999) Global warming in the context of the little ice age. J Geophys Res 104(D16):19057–19070

Gonzalez-Rouco F, von Storch H, Zorita E (2003) Deep soil temperature as proxy for surface air-temperature in a coupled model simulation of the last thousand years. Geophys Res Lett 30:2116

Hughes MK, Diaz HF (1994) Was there a 'medieval warm period', and if so, where and when? Clim Change 26:109–142

Ineson S, Scaife AA, Knight JR, Manners JC, Dunstone NJ, Gray LJ, Haigh JD (2011) Solar forcing of winter climate variability in the northern hemisphere. Nature Geos 4:753–757. doi:10.1038/ngeo1282Received

Lean JL, Rind DH (2008) How natural and anthropogenic influences alter global and regional surface temperature: 1889 to 2006. Geophys Res Lett 35:L18701. doi:10.1029/2008GL034864

Lean J, Beer J, Bradley R (1995) Reconstruction of solar irradiance since 1610: implications for climate change. Geophys Res Lett 22(23):3195–3198

Legutke S, Voss R (1999) The Hamburg atmosphere-ocean coupled circulation model -ECHO-G. Ger Clim Comput Cent (DKRZ) Tech Rep 18:62

Liu J, Wang B, Wang H, Kuang X, Ti R (2009) Forced response of the east asian summer rainfall over the past millennium: results from a coupled model simulation. Clim Dyn 36:323–336. doi:10.1007/s00382-009-0693-6

Mann ME, Bradley RS, Hughes MK (1998) Global-scale temperature patterns and climate forcing over the past six centuries. Nature 392:779–787

Mann ME (2002) Medieval climatic optimum, in Encyclopedia of Global Environmental Change. MacCracken MC, Perry JS (eds), John Wiley, Chichester, pp 514–516

Mann ME, Rutherford S, Wahl E, Ammann C (2007) Robustness of proxy-based climate field reconstruction methods. J Geophys Res Atmos 112:D12109

Mann ME, Zhang Z, Hughes MK, Bradley RS, Miller SK, Rutherford S, Ni F (2008) Proxy-based reconstructions of hemispheric and global surface temperature variations over the past two millennia. PNAS 105(36):13252–13257

Mann ME, Zhang Z, Rutherford S, Bradley RS, Hughes MK, Shindell D, Ammann C, Faluvegi G, Ni F (2009) Global signatures and dynamical origins of the little ice age and medieval climate anomaly. Science 326:1256–1260. doi:10.1126/science.1177303

Meehl GA, Washington WM, Wigley TML, Arblaster JM, Dai A (2003) Solar and greenhouse gas forcing and climate response in the twentieth century. J Climate 16:426–444

Meehl GA, Washington WM, Collins WD, Arblaster JM, Hu A, Buja LE, Strand WG, Teng H (2005) How much more global warming and sea level rise? Science 307:1769. doi:10.1126/science.1106663

Meehl GA, Arblaster JM, Matthes K, Sassi F, van Loon H (2009) Amplifying the pacific climate system response to a small 11-year solar cycle forcing. Science 325:1114–1118. doi:10.1126/science.1172872

Min SK, Legutke S, Hense A, Kwon WT (2005a) Internal variability in a 1000-year control simulation with the coupled climate model ECHO-G—I. Near-surface temperature, precipitation and mean sea level pressure. Tellus 57A:605–621

Min SK, Legutke S, Hense A, Kwon WT (2005b) Internal variability in a 1000-year control simulation with the coupled climate model ECHO-G—II. El Niño Southern Oscillation and North Atlantic Oscillation. Tellus 57A:622–640

Misios S, Schmidt H (2012) Mechanisms involved in the amplification of the 11-year solar cycle signal in the tropical pacific ocean. J Climate. doi:10.1175/JCLI-D-11-00261.1

Reid GC (1997) Solar forcing of global climate change since the mid-17th century. Clim Change 37:391–405

Rind D, Shindell D, Perlwitz J, Lerner J, Lonergan P, Lean J, McLinden C (2004) The relative importance of solar and anthropogenic forcing of climate change between the maunder minimum and the present. J Clim 17:906–929

Robock A, Free M (1996) The volcanic record in ice cores for the past 2000 years.in Climatic Variations and Forcing Mechanisms of last 2000 years. Jones P, Bradley R and Jouzel J, Springer-Verlag, New York, pp 533–546

Scafetta N, West BJ (2006) Phenomenological solar contribution to the 1900–2000 global surface warming. Geophys Res Lett 33:L05708. doi:10.1029/2005GL025539

Schwartz S, Charlson RJ, Kahn RA, Ogren JA, Rodhe H (2010) Why hasn't earth warmed as much as expected? J Clim 23:2453–2464. doi:10.1175/2009JCLI3461.1

Song X, Lubin D, Zhang GJ (2010) Increased greenhouse gases enhance regional climate response to a maunder minimum. Geophys Res Lett 37:L01703. doi:10.1029/2009GL041290

Stocker TF, Qin D, Plattner GK, Tignor M, Allen SK, Boschung J, Nauels A, Xia Y, Bex V, Midgley PM (eds.) IPCC (2013) summary for policymakers. In: climate change 2013: the physical science basis. Contribution of Working Group I to the Fifth Assessment Report of the Intergovernmental Panel on Climate Change. Cambridge University Press, Cambridge and New York

Tett SFB, Stott PA, Allen MR, Ingram WJ, Mitchell JFB (1999) Causes of twentieth-century temperature change near the Earth's surface. Nature 399:569–572

Trenberth KE, Jones PD, Ambenje P, Bojariu R, Easterling D, Klein Tank A, Parker D, Rahimzadeh F, Renwick JA, Rusticucci M, Soden B, Zhai P (2007) Observations: surface and atmospheric climate change. In: climate change 2007: the physical science basis. Contribution of Working Group I to the Fourth Assessment Report of the Intergovernmental Panel on Climate Change (Solomon, S., D. Qin, M. Manning, Z. Chen, M. Marquis, K.B.

Averyt, M. Tignor and H.L. Miller (eds.)). Cambridge University Press, Cambridge and New York

von Storch H, Zorita E, Jones JM, Dmitriev Y, Tett SFB (2004) Reconstructing past climate from noisy data. Science 304:679–682

Xueyuan K, Jian L, Yaocun Z, Danqing H, Ying H (2011) Multi-timescale variation of East Asian Winter Monsoon intensity and its relation with sea surface temperature during last millennium based on ECHO-G simulation. Asia-Pacific J Atmos Sci 47(5):485–495. doi:10.1007/s13143-011-0033-8

Zorita E, González-Rouco F, Legutke S (2003) Testing the Mann et al. (1998) approach to paleoclimate reconstructions in the context of a 1000-yr control simulation with the ECHO-G coupled climate model. J Climate 16:1378–1390

Zorita E, González-Rouco JF, von Storch H, Montávez JP, Valero F (2005) Natural and anthropogenic modes of surface temperature variations in the last thousand years. Geophys Res Lett 32:L08707. doi:10.1029/2004GL021563